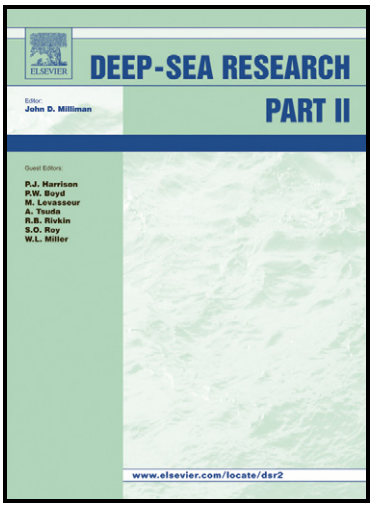

www.elsevier.com/locate/dsr2

Assessing Sub-Antarctic Zone primary productivity from fast repetition rate fluorometry

Wee Cheah, Andrew McMinn, F Brian Griffiths, Karen J Westwood, Simon W Wright, Ernesto Molina, Jason P Webb, Rick van den Enden

PII: S0967-0645(11)00149-4
DOI: doi:10.1016/j.dsr2.2011.05.023
Reference: DSRII 3048

To appear in: *Deep–Sea Research II*

Cite this article as: Wee Cheah, Andrew McMinn, F Brian Griffiths, Karen J Westwood, Simon W Wright, Ernesto Molina, Jason P Webb and Rick van den Enden, Assessing Sub-Antarctic Zone primary productivity from fast repetition rate fluorometry, *Deep–Sea Research II*, doi:10.1016/j.dsr2.2011.05.023

For submission as an article in Deep-Sea Research II, Antarctic biogeochemistry: special issue

Assessing Sub-Antarctic Zone primary productivity from fast repetition rate fluorometry

Wee Cheah[a,b,*], Andrew McMinn[a,b], F. Brian Griffiths[b,c,f] Karen J. Westwood[b,d], Simon W. Wright[b,d], Ernesto Molina[a], Jason P. Webb[e], Rick van den Enden[b,d]

[a] Institute for Marine and Antarctic and Studies, University of Tasmania, Hobart, TAS 7001, Australia.

[b] Antarctic Climate and Ecosystems Cooperative Research Centre, University of Tasmania, Hobart, TAS 7001, Australia.

[c] CSIRO Division of Marine and Atmospheric Research, Hobart, TAS 7000, Australia.

[d] Australian Antarctic Division, Kingston, TAS 7050, Australia.

[e] School of Biological Sciences and Biotechnology, Murdoch University, Murdoch, WA 6150 Australia

[f] Centre for Australian Weather and Climate Research – a partnership of the Bureau of Meteorology and CSIRO

*Corresponding author: wee,cheah@utas.edu.au

Abstract

In situ primary productivity (PP) in the Sub-Antarctic Zone (SAZ) and the Polar Frontal Zone (PFZ) south of Australia was estimated using fast repetition rate fluorometry (FRRF). FRRF-derived PP at Process station 3 (P3) southeast of Tasmania (46°S, 153°E) were higher than P1 in the southwest of Tasmania (46°S, 140°E) and P2 in the Polar Frontal Zone (54°S, 146°E). The FRRF-derived PP rates were well correlated with ^{14}C-uptake rates from one-hour incubations (r^2 = 0.85, slope = 1.23±0.05, P < 0.01, n = 85) but the relationship between both methods differed vertically and spatially. There was a linear relationship between FRRF-based PP and ^{14}C-based PP under light limited conditions in deeper waters. Under light saturated conditions near the surface (0-45 m) the relationship was less clear. This was likely associated with the effects of physiological processes such as cyclic electron flow and the Mehler reaction, which are stimulated at high irradiance. Our results indicate that FRRF can be used to estimate photosynthesis rates in the SAZ and PFZ but to derive an accurate estimation of C-fixation requires a detailed understanding of the physiological properties of the cells and their response to oceanographic parameters under different environmental conditions.

Key words

Fast repetition rate fluorometry; ^{14}C; primary productivity; Sub-Antarctic Zone; Southern Ocean

1. Introduction

The Southern Ocean plays an important role in distributing global nutrients (Sarmiento et al., 2004) and controlling global climate (Sarmiento et al., 1998). The waters of the Southern Ocean are predicted to significantly change in response to climate change (Sarmiento et al., 1998). Climate-driven atmospheric and oceanic changes, which modify the nutrient supply and light regime, are also expected to affect phytoplankton composition dynamics and growth rates in the Southern Ocean. However, the response of phytoplankton to these changes in this region remains unclear (Boyd, 2002).

On site primary productivity (PP) measurements in the Southern Ocean have mostly been carried out using conventional radiocarbon methods (El-Sayed, 2005). The ^{14}C method requires abundant bottle incubations, which are time consuming and labour intensive, and spatially and temporally limited. Remote sensing techniques, which have overcome some of these constraints, have been frequently applied to investigate the spatial and temporal primary production in the Southern Ocean (Sullivan et al., 1993; Arrigo et al., 1998, 2008; Moore and Abbott, 2000) but the limited number of *in situ* measurements available for large areas of the Southern Ocean has hindered the sea truth validation and interpretation of estimates from satellite imagery.

The fast repetition rate fluorometry (FRRF) technique, which was only introduced in the last decade, has been applied widely to study the photosynthesis of phytoplankton in the ocean (Suggett et al., 2005). Based on variable chlorophyll *a* (chl *a*) fluorescence, the FRRF provides *in situ* non-destructive, instantaneous measurements of photosynthetic parameters and allows both the derivation of gross primary production at fixed depth and continuous observations with a temporal resolution of seconds

(Falkowski and Kolber, 1995). Attempts to determine the reliability of the FRRF in estimating PP have been carried out in several different regions. These studies, in either highly productive regions (Suggett et al., 2001; Moore et al., 2003; Raateoja et al., 2004; Smyth et al., 2004; Estevez-Blanco et al., 2006; Melrose et al., 2006) or oligotrophic waters (Corno et al., 2006) found significant correlations between FRRF measurements and traditional radiocarbon derived estimates. However, the relationship between the two methods is not consistent. The inconsistencies are thought to be linked to differences in how the two techniques estimate PP. The ^{14}C method measures the uptake and assimilation of dissolved inorganic carbon whilst the FRRF measurement is equivalent to gross oxygen evolution based on the electron transport rate in photosystem II (PSII) (Suggett et al., 2001). As a bio-optical instrument, FRRF measures instantaneous photosynthesis in the water column that reflects real-time irradiance, whilst ^{14}C uptake rates are a product of incubations integrated over a certain period of time that are subjected to average irradiance. Several key assumptions (e.g. photosynthetic unit size, maximum quantum yield of electron transport and photosynthetic quotient) are required in the FRRF-based PP model and these have been found to vary between different water bodies (Falkowski and Kolber, 1995).

Previous applications of FRRF in the Southern Ocean were mainly focused on the physiological conditions of phytoplankton in response to nutrients (Olson et al., 2000; Strutton et al., 2000; Boyd and Abraham, 2001; Gervais et al., 2002; Vaillancourt et al., 2003; Holeton et al., 2005). So far, there have been no published studies on the use of the FRRF to derive phytoplankton productivity in the Southern Ocean, despite its flexibility. In this study, we present PP data collected from the Sub-Antarctic Zone (SAZ), which lies between the Subtropical Front (STF) and the Sub-Antarctic Front (SAF) (Fig. 1), south of Tasmania using both the FRRF and ^{14}C techniques. This region, which is reported to be a large sink for atmospheric CO_2 (Metzl et al., 1999; McNeil et al., 2001), has a high degree of spatial and temporal

variability in water properties. The mixed layer south of SAZ, for instance, is lower in temperature and salinity but higher in nutrients than that to the north (Rintoul and Trull, 2001). By comparing the FRRF technique with the ^{14}C technique, we assess the reliability of FRRF-derived PP for this region.

2. Materials and methods

2.1. Sampling

FRRF and ^{14}C measurements were obtained from the SAZ south of Australia (43°-55° S, 140°-154° E) during the Sub-Antarctic Zone Sensitivity to Environmental Change (SAZ-Sense) survey. The voyage was conducted aboard RSV *Aurora Australis* from 17 January to 20 February 2007 and consisted of three process (P) stations and 24 transit (T) stations. For the purpose of this study, a total of 11 stations were investigated, at which there were 14 conductivity-temperature-depth (CTD) casts and FRRF deployments (Table 1). Water samples for ^{14}C uptake, chl *a* concentration and other hydrological measurements were collected from Niskin bottles alongside CTD casts. A Fast*tracka* FRR fluorometer (Chelsea Instruments, UK) integrated with a photosynthetically active radiation (PAR, 400 -700 nm) radiometer and a pressure sensor were deployed immediately after CTD casts with both light and dark chambers facing upward to a final depth of ca. 100 m at a vertical rate ≤ 0.5 m s^{-1}. The vessel was re-orientated to avoid ship shadow prior to each FRRF deployment.

2.2. FRRF measurements

FRRF fluorescence yields were measured using an inbuilt protocol that provided a flash sequence consisting of a series of 100 subsaturation flashlets (1.1 μs flash duration and 2.8 μs inter flash

period) and a series of 20 relaxation flashlets (1.1 μs flash duration and 51.6 μs inter flash period) with the gain set in autoranging mode. Fluorescence transients obtained at each deployment were then fitted to the biophysical model of Kolber et al. (1998) using post-processing software (v 1.8) provided by Chelsea Instruments. The parameters derived were minimum (F_o) and maximum (F_m) fluorescence, variable fluorescence (F_v), maximum photochemical efficiency (F_v/F_m), effective absorption cross section of PSII (σ_{PSII}) in darkness and under actinic light (F', F_m', F_q', F_q'/F_m', σ_{PSII}'). Parameters and definitions used in this study are reported in Table 2. Data were quality controlled by recalculating the F_o, F_m, F' and F_m' after subtracting the mean of the blank and were aggregated over 2 m intervals. Data with PAR ≤ 0 and depth ≤ 0 were excluded. The blank sample was obtained from filtered seawater (0.2 μm) collected from 6 m depth.

2.3. ^{14}C measurements

The ^{14}C productivity method was based on the small bottle ^{14}C technique (Lewis and Smith, 1983) as detailed by Westwood et al. (this issue). In brief, 400 ml water samples were collected from six to seven depths, depending on the mixed layer depth of the station. The water samples were stored in darkened polycarbonate jars in a seawater-cooled, insulated container, until the commencement of incubations. Each jar was spiked with 6.327 x 10^6 Bq (0.171 mCi) $NaH^{14}CO_3$ to produce a working solution of 39.183 x 10^3 Bq per ml (1.1 μCi ml^{-1}). Seven ml aliquots of working solution were then added to transparent glass scintillation vials and incubated for 1 hour at 21 light intensities ranging from 0 to 416 μmol photons m^{-2} s^{-1}. The illumination was provided by GE polylux XL F58W/860 fluorescent lamps filtered through CT blue filters with wavelength centered at around 435 nm. After acidification and venting to remove excess $NaH^{14}CO_3$, 10 ml Aquassure scintillation fluid was added and the samples were

counted using a Packard TriCarb 2900 TR scintillation counter with the maximum counting time set at 5 min.

Photosynthesis-irradiance (P-E) relationships were then calculated and the equation of Platt et al. (1980) was used to fit curves to data using least squares non-linear regression:

$$P^{\mathrm{B}} = P_{\max}[(1-e^{-\alpha E/P_{\max}})(e^{-\beta E/P_{\max}})]$$

Where P^{B} is the carbon fixation rates per unit chl *a* at a given light intensity [mg C (mg chl *a*)$^{-1}$ h^{-1}], $P_{\max}$ is the light-saturated photosynthetic rate [mg C (mg chl *a*)$^{-1}$ h^{-1}], α is the initial slope of the light-limited section of the P-E curve [mg C (mg chl *a*)$^{-1}$ h^{-1} (µmol photons m^{-2} s^{-1})$^{-1}$], *E* is the irradiance (µmol photons m^{-2} s^{-1}) and β is the photoinhibition parameter where applicable [mg C (mg chl *a*)$^{-1}$ h^{-1} (µmol photons m^{-2} s^{-1})$^{-1}$]. P^{B} was then multiplied by the chl *a* concentration at depth *z* to obtain ^{14}C primary productivity estimates ($P_{14\mathrm{C}}(z)$, mmol C m^{-3} h^{-1}).

$$P_{14C}(z) = P^{\mathrm{B}}(z) \times \mathrm{chl}\ a$$

To minimise variability between the ^{14}C and FRRF productivity estimates, *in situ* irradiance measurements at depth, $E(z)$, was obtained from the FRRF PAR sensor. Chl *a* concentrations were determined by filtering the seawater samples through 13 mm diameter Whatman GF/F filters and frozen immediately in liquid nitrogen for later analysis using the high performance liquid chromatography (HPLC) method (see Wright et al. (2010) for details).

2.4. FRRF primary productivity model

In situ chlorophyll *a*-specific rate of electron transfer, $ETR^{chl}(z)$ [mmol electron (mg chl *a*)$^{-1}$ h^{-1}] at each depth was determined by substituting the PSII parameters into the following equation (Suggett et al., 2005):

$$ETR^{chl} = E(z)\ \sigma_{PSII}'(z)\ n_{PSII}\ \ q_P\ \times 0.0243 \qquad (1)$$

Where E is the irradiance (µmol photons m^{-2} s^{-1}), σ_{PSII}' is the effective absorption cross section under actinic light (Å^2 quanta^{-1}), n_{PSII} is the photosynthetic unit size of PSII [mol RCII (mol chl *a*)$^{-1}$] and is set at 0.002 (Falkowski and Kolber, 1995) based on the characteristics of eukaryotes which dominate this area, q_P is the photochemical quenching ($F_q'/F_v' = F_m' - F'/F_m'/F_o'$). The constant 0.0243 included conversion from seconds to hours, µmol electron to mol electron and Å^2 quanta^{-1} to m^2 mol RCII^{-1}, and mol chl *a* to mg chl *a*.

In order to compare with ^{14}C carbon fixation rates, equation (1) needs to be modified into:

$$P_{FRRF}(z) = E(z)\ \sigma_{PSII}'(z)\ n_{PSII}\ \ q_P\ \ 1/k\ \ \text{chl}\ a\ \text{x}\ 0.0243 / \text{PQ} \qquad (2)$$

Where P_{FRRF} is the FRRF-derived primary productivity (mmol C m^{-3} h^{-1}), *1/k* is the quantum yield of electron transport through PSII per O_2 molecule evolved [mol O_2 (mol electron)$^{-1}$] and is assumed at 0.25. Chl *a* is the chl *a* concentration (mg chl *a* m^{-3}), PQ is the photosynthetic quotient [mol O_2 evolved (mol CO_2 incorporated)$^{-1}$] with a value of 1.4 based the assumption that growth to be mostly nitrate-derived (Laws, 1991).

2.5 Data analysis

A geometric mean regression (model II) regression of FRRF- and ^{14}C based PP was applied to determine the slope coefficient and intercept of this relationship. Analysis of variance (ANOVA) was used to determine significant differences between the FRRF-based PP: ^{14}C-based PP ratio for all data, light limited data and light saturated data. The differences between the ratios for the three process stations were also analysed. A Pearson's correlation analysis was performed to analyse the relationship between the ratios and environmental variables (i.e. temperature, salinity, nitrite + nitrate, phosphate, silicate and iron) and species composition.

3. Results

3.1. Hydrological conditions

This study covered an area that consisted of several different water masses with variable physical and biological characteristics. Sea surface temperature (SST) at Process station 1 (P1, SAZ-West) ranged from 12.8 °C to 13.1 °C with a salinity of approximately 34.7. The mixed layer (ML) depths in this area ranged from 25 m to 46 m. SST and salinity at Process station 3 (P3, SAZ-East) were approximately 13.5 °C and 35.0 respectively. Two MLs was present at P3, a shallow ML from the surface to 16 m and another ML at 70 m. Process station 2 (P2) in the PFZ showed lower SST (5.5 °C) and salinity (33.8) than water in the SAZ and had a mixed layer depth of 49 m. A deep mixed layer was found at transit station 3 (Table 1). Physical characteristics of the upper water column in the sampling area are discussed in detail by Bowie et al. (this issue).

3.2. Variable fluorescence measurements

The maximum (F_v'/F_m') and effective (F_q'/F_m') photochemical quantum efficiency of PSII in the SAZ ranged from 0.14 to 0.55 and 0.03 to 0.54, respectively. F_v'/F_m' were lowest at P2 with surface values < 0.20 and higher at P1 and P3 (surface values ~0.35 ~ 0.40, respectively). The highest F_v'/F_m' recorded at P2 was 0.35, 0.45 at P1 and 0.47 at P3. The vertical distribution of F_v'/F_m' and F_q'/F_m' at P1 and P3 was low at the surface, increased with depth and then decreased slightly at greater depths (> 70 m) with the exception of P2, where an increase in F_v'/F_m' and F_q'/F_m' was observed at ~ 100 m. The strongly quenched F_q'/F_m' leads to a divergence between F_v'/F_m' and F_q'/F_m' at the surface, with F_v'/F_m' higher than F_q'/F_m' (Fig. 2a & c). The divergence disappeared at ca. 40 m. The effective cross section of PSII in darkness (σ_{PSII}) and under ambient light (σ_{PSII}') varied from 160 to 811 and 153 to 904Å^2 quanta^{-1}, respectively. Both σ_{PSII} and σ_{PSII}' demonstrated a similar vertical pattern to F_q'/F_m'. In contrast to photochemical efficiency values, σ_{PSII}' was generally higher than σ_{PSII}. The photochemical quenching (q_P) showed a low surface value, varied between 0.06 and 0.40 in the first 20 m of the water column, and then increased steadily with depth (Fig. 2a & c).

3.3. Chlorophyll a, productivity and macronutrients

Total chlorophyll *a* (chl *a*) concentrations were generally high in surface waters in this study and ranged from 0.11 to 1.85 mg chl *a* m^{-3}. Chl *a* concentrations in the surface waters at P1 and P2 were generally < 1.0 mg chl *a* m^{-3}, while P3 demonstrated values > 1.0 mg chl *a* m^{-3} (Fig. 3a). The maximum chl *a* concentration (2.49 mg chl *a* m^{-3}) was found at a depth of 29 m at CTD 91. Surface primary productivity (PP) estimated from the FRRF in this study ranged from 0.26 to 5.65 mmol C m^{-3} h^{-1}, while for the ^{14}C method estimates, PP ranged from 0.19 to 4.20 mmol C m^{-3} h^{-1}. Both FRRF and ^{14}C methods showed higher PP at P1 and P3 than P2, with the maximum PP value recorded at P3 (CTD 77) off eastern

Tasmania (Table 1). The vertical distribution of PP generally followed the distribution pattern of chl *a* concentration but without a production maximum in deeper waters (Fig. 3b).

Concentrations for nitrate + nitrite and phosphate demonstrated similar patterns with values ranging from 0.1-17.3 µmol L^{-1} and 0.4-1.1 µmol L^{-1} at P1 and P3 (SAZ), 23.8-30.2 µmol L^{-1} and 1.6-2.3 µmol L^{-1} at P2 (PFZ). Surface (0-20 m) nitrate + nitrite concentrations were high at P2 (25 µmol L^{-1}), and low at P1 (0.5 µmol L^{-1}) and P3 (0.4 µmol L^{-1}). Surface phosphate concentrations at P2 (1.5 µmol L^{-1}) were also higher than P1 (0.5 µmol L^{-1}) and P3 (0.45 µmol L^{-1}). Silicate concentrations were low at all three process stations with surface value < 1 µmol L^{-1} (Fig. 3d-f).

3.4. FRRF and ^{14}C primary productivity estimates

There was a significant correlation between FRRF- and ^{14}C-derived PP estimates (r^2 = 0.85, slope = 1.23±0.05 s.d., p < 0.01, n = 85) (Fig. 4a). This indicates that the FRRF method was measuring similar PP changes to the ^{14}C method. When only measurements from light-limited depths are compared (below saturating irradiance value, $E_k = P_{max}/\alpha$), the relationship improved (r^2 = 0.96 and a slope = 1.05±0.03 s.d., P < 0.01, n = 71) (Fig. 4b). At light-saturated depths (above E_k value) the correlation was poorer (r^2 = 0.64 and the slope = 1.43±0.23s.d., P < 0.01, n = 14) (Fig. 4c). There was also a significant correlation between chl *a*-specific rate of electron transfer (ETR^{chl}) and carbon uptake rate per unit chl *a*, P^B [in mmol C (mg chl *a*)$^{-1}$ h^{-1}] but the relationship was less well correlated (r^2 = 0.74, slope = 5.07±0.28 s.d., P < 0.01, n = 85) (Fig. 5a). A significant relationship was also found between the light normalised FRRF-based PP and ^{14}C-based PP (r^2 = 0.86, slope = 1.03±0.00 s.d., P < 0.01, n = 85) (Fig. 5b). FRRF-derived PP at P1 underestimated ^{14}C-uptake rates (r^2 = 0.98, slope = 0.79±0.06 s.d., P < 0.01, n = 19) (Fig. 6a) whilst FRRF-

derived PP were higher than ^{14}C-based PP at P2 (r^2 = 0.97, slope = 1.67±0.11 s.d., P < 0.01, n = 6) and P3 (r^2 = 0.92, slope = 1.43±0.10 s.d., P < 0.01, n = 14) (Fig. 6b & c).

4. Discussion

4.1. Variability of fluorescence measurements

The fluorescence parameters exhibit a close relationship with the light levels and nutrients. The reduction in both the photochemical efficiency (F_v'/F_m' and F_q'/F_m') at the surface during midday implies the effects of non-photochemical quenching (q_N) at high irradiances (Fig. 2c). At high light, q_N acts as a self-protection mechanism that dissipates excess light energy in the form of heat, rather than in the form of fluorescence to avoid photodamage (Falkowski and Raven, 2007). The divergence between F_v'/F_m' and F_q'/F_m' in surface waters shows that the short periods of dark-adaptation in the dark chamber allows the reoxidation of Q_A in the reaction centres with a time constant of milliseconds (Kolber and Falkowski, 1993). This resulted in the relaxation of photochemical quenching (q_P) and a higher value of F_v'/F_m' than F_q'/F_m' which is influenced by both q_N and q_P. In the effective absorption cross section of PSII, the quenching occurs in the antenna pigments where the relaxation time scale ranges from 5-60 min (Olaizola and Yamamoto, 1994), which caused the decrease in both σ_{PSII} and σ_{PSII}' at the surface at high irradiances.

When the irradiances were low enough at depth (ca. 50 m) where the effect of non-photochemical quenching could be neglected, F_v/F_m values were found to respond to dissolved iron (dFe) concentrations. At P1 and P3, F_v/F_m were 0.38 and 0.44 with dFe levels 0.27 and 0.41 nmol L^{-1}, respectively. Low F_v/F_m (0.28) at P2 was found to correspond to a low dFe concentration (0.19 nmol L^{-1}).

An increase in F_v/F_m (0.30) at ca. 100 m at P2 was consistent with higher dFe levels (0.25 nmol L^{-1}) at this depth (Bowie et al., 2009; Lannuzel et al., this issue). This indicates that the phytoplankton in the PFZ were likely to be suffering from Fe limitation.

4.2. Primary productivity SAZ-West, SAZ-East and PFZ

Total chlorophyll *a* (chl *a*) concentration and primary productivity (PP) measurements observed in this study are consistent with other studies carried out in this area (Sedwick et al., 1997; Griffiths et al., 1999) although chl *a* concentration was higher than in the measurements made by Wright et al. (1996) in austral autumn. Wright et al. (1996) obtained relatively low chl *a* concentrations ranging between 0.08 and 0.25 mg chl *a* m^{-3}. The higher concentrations of chl *a* and rates of PP recorded in the SAZ than in the PFZ is consistent with low concentrations of nitrate + nitrite and phosphate at P1 and P3, but higher at P2. This indicates that macronutrient drawdown occurs in the SAZ but not in the PFZ, which is likely due to Fe limitation in this region. The depletion of silicate in surface waters at all stations implies that this area might be silicate-limited (Hutchins et al., 2001).

The differences between the ratios of FRRF- and ^{14}C-based PP estimates of P1 (SAZ-West), P2 (PFZ) and P3 (SAZ-East) were not significant, suggesting that environmental variable do not significantly influence the relationship between the FRRF- and ^{14}C-based PP. This was confirmed by the Pearson's correlation analysis, which showed no significant relationship between the PP ratio and the environmental variables (i.e. temperature, salinity, nitrite + nitrate, phosphate, silicate and iron). Similar results were also obtained from an analysis of the correlation between the ratios and major

phytoplankton groups (e.g. diatom, dinoflagellate, haptophyte and cyanobacteria), which indicate that the species composition did not significantly influence the FRRF and ^{14}C relationship.

4.3. FRRF- and ^{14}C-based productivity

The strongly significant relationship between FRRF and ^{14}C estimates indicates that both methods approximate similar PP changes across different levels of productivity. FRRF-based PP measurements overestimated the ^{14}C-uptake rates by a factor of 1.23 (Fig. 3a). This value is well within the range of other published results, which are mostly between 0.5 and 2.0. Kolber and Falkowski (1993) obtained a slope of 1.06 between these estimates using the pump and probe technique (predecessor of FRRF). Using the same technique, Boyd et al. (1997) obtained fluorescence-based PP estimates that were 0.5 lower than the Kolber and Falkowski (1993) ratio. Estimates of PP from FRRF by other groups (Suggett et al., 2001; Moore et al., 2003; Raateoja et al., 2004; Corno et al., 2006; Estevez-Blanco et al., 2006) were 1.4 to 2.0 higher than those estimated from the ^{14}C method. In contrast, Smyth et al. (2004) and Melrose et al. (2006) obtained FRRF-based PP that underestimated ^{14}C-uptake rates by 0.6 to 0.8. However, it should be noted that different measurement units and incubation times that were used in the estimation of ^{14}C-based PP in these studies, complicates the comparison.

When measurements of PP below light saturation (E_k) were considered, the divergence between estimates from FRRF and ^{14}C decreased. The slope value dropped from 1.43 (r^2 = 0.64) in light-saturated measurements (Fig. 4c) to 1.05 (r^2 = 0.96) in light-limited measurements (Fig. 4b). Both field (Raateoja et al., 2004; Corno et al., 2006) and laboratory (Fujiki et al., 2007) experiments have shown that at high actinic light levels, the relationship between FRRF- and ^{14}C-based estimates is non-linear. This is

probably due to the effects of physiological processes such as cyclic electron flow, the Mehler reaction and photorespiration, all of which are stimulated at high light levels. At supra-optimal light intensities, photon absorption by PSII approaches the capacity of the electron transport system leading to the cyclic electron flow around PSII with some electrons returned from the acceptor side (PQH_2) of PSII to the donor side (Z) through cytochrome *b*559 (Falkowski et al., 1986). Cyclic electron flow is stimulated at light saturation when the plastoquinone pool is reduced (Prasil et al., 1996). It is estimated that ~15% of total electron transport in PSII flows from the acceptor side to its donor side under light saturated conditions (Falkowski et al., 1986) and this would therefore produce an FRRF-based estimate that is up to 15% greater than a ^{14}C-based estimate and is consistent with the measurements documented here. A recent study by Bailey et al. (2008) demonstrated that marine cyanobacteria in the oligotrophic waters extract significant amounts of electron from the electron transport chain, donating them to O_2 by way of a propyl gallate-sensitive oxidase to alleviate excessive PSII excitation pressure. In the Mehler reaction, reduced ferredoxin on the acceptor side of PSI donates electrons to O_2 molecules that are generated by the oxidation of water rather than the usual terminal electron acceptor NADP+ in the photosynthetic electron transport chain (Heber, 2002). The Mehler reaction is thought to redirect ~10% to 50% of total electron transport and is less important under light limiting conditions (Kana, 1992, 1993). In addition to cyclic electron flow and the Mehler reaction, photorespiration is also thought to affect the rate of C fixation. However, photorespiration is usually low in aquatic photoautotrophs (Falkowski and Raven, 2007) and considered to be less important (Ogren, 1984).

Differences between PP estimates at high light may also be due to different lengths of incubation period. Most ^{14}C PP measurements have incubation periods of between 1 and 10 hours, longer incubation periods allow significant leakage of respired carbon and dissolved organic carbon

(DOC), and leads to an under estimate of PP. In the ^{14}C technique, cells are only subjected to the average irradiance over the incubation period and with no vertical mixing, create a potentially unrealistic photoacclimation and photoinhibition state (Gallegos and Platt, 1985). These factors, therefore, are likely to affect the photosynthesis-irradiance curve (Flameling and Kromkamp, 1997; Macedo et al., 2002). The FRRF measurement period has a resolution of seconds, and measurements are sensitive to short-term variability in the underwater light field caused by surface waves, internal waves, convection, circulation, cloud coverage, etc., which impose a fluctuating light environment on the phytoplankton. In addition, Raateoja et al. (2004) reported that near surface, scattered ambient red light can reach the FRRF detector and flatten the variable fluorescence transients, which could affects the reliability of the near-surface data. Care should thus be taken when interpreting this data. For our study, it was difficult to quantify the influence of the red light but noisy near the surface data has been excluded.

Differences between PP estimates by FRRF and ^{14}C techniques can be attributed to the fact that each uses a different methodology (electron transport rates and carbon incorporation) and consequently measures different attributes of photosynthesis. Physiological processes such as those mentioned above, as well as other metabolic activities (e.g. nutrient uptake, reproduction), may influence the relationship between FRRF and ^{14}C. These processes could result in an increase in the number of electrons transported through PSII for each molecule of CO_2 fixed, as suggested by the non-linear relationship between the chl *a*-specific rate of electron transfer (ETR^{chl}) and carbon uptake rate per unit chl *a*, P^B (r^2 = 0.74, slope = 5.07, $P < 0.01$, n = 85) (Fig. 5a). There are also uncertainties associated with the assumed values of n_{PSII} and PQ, and errors in estimating σ_{PSII}'. The n_{PSII}, which is difficult to measure especially in the field ranges from 0.001 to 0.007 mol RCII (mol chl *a*)$^{-1}$ in cultured samples (Falkowski et al., 1981; Barlow and Alberte, 1985) whilst PQ is found to vary from 1.1 to 1.5 in

the world oceans (Laws, 1991). Furthermore, the σ_{PSII}' used in this study was not corrected for variability in the spectral quality of the *in situ* light field. Suggett et al. (2001) and Raateoja et al. (2004) reported that measured σ_{PSII}' overestimated the actual σ_{PSII}' by 8 to 69 % in case 2 waters. However, this uncertainty has yet to be quantified in case 1 waters such as in this study area. Overall, variability in n_{PSII}, PQ and σ_{PSII}' could accounts for up to 30 % of the potential uncertainty in estimates of PP using the FRRF technique.

The better relationship between FRRF- and ^{14}C-derived PP obtained in this study compared to many others can probably be explained by the much shorter ^{14}C incubation times used in this study. The ^{14}C incubation time used here was of short duration (one hour $\pm$ 5 minutes) compared with times of >1 h used in other studies (Raateoja et al., 2004; Corno et al., 2006; Estevez-Blanco et al., 2006). Measuring the whole, acidified sample means any ^{14}C-DOC released by the cells is also included in the gross PP estimate. Thus, we suggest that our ^{14}C measurements more closely approximate gross primary production than net primary production, although some studies suggest that the ^{14}C technique can approximate net carbon fixation even with short incubation times (Williams et al., 1996; Marra, 2002). It is also felt that the photosynthetic quotient (PQ=1.4) and photosynthetic unit size (n_{PSII}=0.002) used in this study are appropriate for this area and by using q_P (F_q'/F_v') and σ_{PSII}' in the FRRF PP model the effect of non-photochemical quenching has been included. While a spectral correction was not made, the light normalised data comparisons (Fig. 5b) showing a close relationship between the FRRF- and ^{14}C-based PP, suggest that the FRRF excitation flashes (centred at 478 nm) and the light source used in the ^{14}C incubation (centred at 435 nm) provide the resident cells with a similar excitation spectrum and this may explain the similar PP estimates by both methods.

Conclusion

This study provides both validation and constraints for determining gross primary productivity (GPP) by FRRF in the Southern Ocean. The FRRF can provide *in situ* measurements of photosynthesis parameters at a much higher frequency than conventional radiocarbon techniques and can be applied to moorings as well as to remote surveillance. These characteristics make the FRRF a convenient tool in oceanographic research, especially in the vast and remote Southern Ocean. However, although strong correlations with ^{14}C uptake rates were found in this study, the reliability of FRRF in measuring PP is hindered by several factors such as uncertainties in several key assumptions.

Acknowledgement

We would like to thank the captain and crew of RSV *Aurora Australis*, Australian Antarctic Division's gear officers, the CTD team and fellow expeditioners for their support during the cruise. We are indebted to Mark Rosenberg for the oceanography data, and Neil Johnson and Alicia Navidad for the nutrients data. We would also like to thank Philip Boyd (NIWA) and Klaus Meiners (ACE CRC) and four anonymous reviewers for their comments on the manuscript. This work was supported financially by the Australian Government through the Australian Antarctic Science Grants (AAS) Project #2720 and Antarctic Climate and Ecosystems Cooperative Research Centres (ACE CRC). Wee Cheah was supported by a scholarship from the ACE CRC.

References

Arrigo, K.R., Worthen, D., Schnell, A., Lizotte, M.P., 1998. Primary production in Southern Ocean waters. J. Geophys. Res. 103, 15587-15600, doi:10.1029/98JC00930.

Arrigo, K.R., van Dijken, G.L., Bushinsky, S., 2008. Primary production in the Southern Ocean, 1997-2006. J. Geophys. Res. 113, C08004, doi:10.1029/2007JC004551.

Bailey, S., Melis, A., Mackey, K.R.M., Cardol, P., Finazzi, G., van Dijken, G., Berg, G.M., Arrigo, K., Shrager, J., Grossman, A., 2008. Alternative photosynthetic electron flow to oxygen in marine *Synechococcus*. Biochim. Biophys. Acta 1777, 269-276, 10.1016/j.bbabio.2008.01.002.

Barlow, R.G., Alberte, R.S., 1985. Photosynthetic characteristics of phycoerythrin-containing marine *Synechococcus* spp. I. Responses to growth photon flux density. Mar. Biol. 86, 63-74, doi: 10.1007/BF00392580.

Bowie, A.R., Lannuzel, D., Remenyi, T.A., Wagener, T., Lam, P.J., Boyd, P.W., Guieu, C., Townsend, A.T., Trull, T.W., 2009. Biogeochemical iron budgets of the Southern Ocean south of Australia: Decoupling of iron and nutrient cycles in the subantarctic zone by the summertime supply. Global Biogeochem. Cycles 23, GB4034, doi:10.1029/2009GB003500.

Bowie, A.R., Griffiths, F.B., Dehairs, F. and Trull, T.W., 2011. Oceanography of the subantarctic and polar frontal zones south of Australia during summer: setting for the SAZ-Sense study. Deep-Sea Res. Pt. II, this isuue.

Boyd, P.W., 2002. Environmental factors controlling phytoplankton processes in the Southern Ocean. J. Phycol. 38, 844-861, doi: 10.1046/j.1529-8817.2002.t01-1-01203.x.

Boyd, P.W., Abraham, E.R., 2001. Iron-mediated changes in phytoplankton photosynthetic competence during SOIREE. Deep-Sea Res. Pt. II 48, 2529-2550, doi: 10.1016/S0967-06450100007-8.

Boyd, P.W., Aiken, J., Kolber, Z., 1997. Comparison of radiocarbon and fluorescence based (pump and probe) measurements of phytoplankton photosynthetic characteristics in the Northeast Atlantic Ocean. Mar. Ecol. Prog. Ser. 149, 215-226, doi: 10.3354/meps149215.

Corno, G., Letelier, R.M., Abbott, M.R., Karl, D.M., 2006. Assessing primary production variability in the North Pacific subtropical gyre: A comparison of fast repetition rate fluorometry and ^{14}C measurements. J. Phycol. 42, 51-60, doi: 10.1111/j.1529-8817.2006.00163.x.

El-Sayed, S.Z., 2005. History and evolution of primary productivity studies of the Southern Ocean. Polar Biol. 28, 423-438, doi: 10.1007/s00300-004-0685-2.

Estevez-Blanco, P., Cermeno, P., Espineira, M., Fernandez, E., 2006. Phytoplankton photosynthetic efficiency and primary production rates estimated from fast repetition rate fluorometry at coastal embayments affected by upwelling (Rias Baixas, NW of Spain). J. Plankton Res. 28, 1153-1165, doi: 10.1093/plankt/fbl046.

Falkowski, P.G., Fujita, Y., Ley, A., Mauzerall, D., 1986. Evidence for cyclic electron flow around photosystem II in *Chlorella pyrenoidosa*. Plant Physiol. 81, 310-312, doi: 10.1104/pp.81.1.310.

Falkowski, P.G., Kolber, Z., 1995. Variations in chlorophyll fluorescence yields in phytoplankton in the world oceans. Aust. J. Plant Physiol. 22, 341-355, doi: 10.1071/PP9950341.

Falkowski, P.G., Owens, T.G., Ley, A.C., Mauzerall, D.C., 1981. Effects of growth irradiance levels on the ratio of reaction centers in two species of marine-phytoplankton. Plant Physiol. 68, 969-973, doi: 10.1104/pp.68.4.969.

Falkowski, P.G., Raven, J.A., 2007. Aquatic photosynthesis, second ed. Princeton University Press, Princeton.

Flameling, I.A., Kromkamp, J., 1997. Photoacclimation of *Scenedesmus protuberans* (Chlorophyceae) to fluctuating irradiances simulating vertical mixing. J. Plankton Res. 19, 1011-1024, doi: 10.1093/plankt/19.8.1011.

Fujiki, T., Suzue, T., Kimoto, H., Saino, T., 2007. Photosynthetic electron transport in *Dunaliella tertiolecta* (Chlorophyceae) measured by fast repetition rate fluorometry: relation to carbon assimilation. J. Plankton Res. 29, 199-208, doi: 10.1093/plankt/fbm007.

Gallegos, C.L., Platt, T., 1985. Vertical advection of phytoplankton and productivity estimates: A dimensional analysis. Mar. Ecol. Prog. Ser. 26, 125-134.

Gervais, F., Riebesell, U., Gorbunov, M.Y., 2002. Changes in primary productivity and chlorophyll a in response to iron fertilization in the Southern Polar Frontal Zone. Limnol. Oceanogr. 47, 1324-1335.

Griffiths, F.B., Bates, T.S., Quinn, P.K., Clementson, L.A., Parslow, J.S., 1999. Oceanographic context of the First Aerosol Characterization Experiment (ACE 1): A physical, chemical, and biological overview. J. Geophys. Res. 104, 21649-21671, doi: 10.1029/1999JD900386.

Heber, U., 2002. Irrungen, Wirrungen? The Mehler reaction in relation to cyclic electron transport in C3 plants. Photosynth. Res. 73, 223-231, doi: 10.1023/A:1020459416987.

Holeton, C.L., Nedelec, F., Sanders, R., Brown, L., Moore, C.M., Stevens, D.P., Heywood, K.J., Statham, P.J., Lucas, C.H., 2005. Physiological state of phytoplankton communities in the Southwest Atlantic sector of the Southern Ocean, as measured by fast repetition rate fluorometry. Polar Biol. 29, 44-52, doi: 10.1007/s00300-005-0028-y.

Hutchins, D.A., Sedwick, P.N., DiTullio, G.R., Boyd, P.W., Queguiner, B., Griffiths, F.B., Crossley, C., 2001. Control of phytoplankton growth by iron and silicic acid availability in the subantarctic Southern Ocean: Experimental results from the SAZ Project. J. Geophys. Res. 106, 31559-31572, doi: 10.1029/2000JC000333.

Kana, T.M., 1992. Relationship between photosynthetic oxygen cycling and carbon assimilation in *Synechococcus* WH7803 (Cyanophyta). J. Phycol. 28, 304-308, doi: 10.1111/j.0022-3646.1992.00304.x.

Kana, T.M., 1993. Rapid oxygen cycling in *Trichodesmium thiebautii*. Limnol. Oceanogr. 38, 18-24.

Kolber, Z., Falkowski, P.G., 1993. Use of active fluorescence to estimate phytoplankton photosynthesis in situ. Limnol. Oceanogr. 38, 1646-1665.

Kolber, Z.S., Prasil, O., Falkowski, P.G., 1998. Measurements of variable chlorophyll fluorescence using fast repetition rate techniques: defining methodology and experimental protocols. Biochim. Biophys. Acta 1367, 88-106, doi: 10.1016/S0005-2728(98)00135-2.

Lannuzel, D., Remenyi, T., Lam, P., Townsend, A., Ibisanmi, E., Butler, E., Wagener, T., Schoemann, V., Bowie, A.R., 2011. Distributions of dissolved and particulate iron in the sub-Antarctic and Polar Frontal Southern Ocean (Australian sector). Deep-Sea Res. Pt. II, this issue.

Laws, E.A., 1991. Photosynthetic quotients, new production and net community production in the open ocean. Deep-Sea Res. Pt. I 38, 143-167, doi: 10.1016/0198-01499190059-O.

Lewis, M.R., Smith, J.C., 1983. A small volume, short-Incubation-time method for measurement of photosynthesis as a function of incident irradiance. Mar. Ecol. Prog. Ser. 13, 99-102.

Macedo, M.F., Duarte, P., Ferreira, J.G., 2002. The influence of incubation periods on photosynthesis-irradiance curves. J. Exp. Mar. Biol. Ecol. 274, 101-120, doi: 10.1016/S0022-0981(02)00202-2.

Marra, J., 2002. Approaches to the measurement of plankton production, in: Williams, P.J.B., Thomas, D.N., Reynolds, C.S. (Eds.), Phytoplankton productivity. Blackwell Science Ltd., Oxford, pp. 78-108.

McNeil, B.I., Tilbrook, B., Matear, R.J., 2001. Accumulation and uptake of anthropogenic CO_2 in the Southern Ocean, south of Australia between 1968 and 1996. J. Geophys. Res. 106, 31431-31445, doi: 10.1029/2000jc000331.

Melrose, D.C., Oviatt, C.A., O'Reilly, J.E., Berman, M.S., 2006. Comparisons of fast repetition rate fluorescence estimated primary production and ^{14}C uptake by phytoplankton. Mar. Ecol. Prog. Ser. 311, 37-46, doi: 10.3354/meps311037.

Metzl, N., Tilbrook, B., Poisson, A., 1999. The annual fCO_2 cycle and the air-sea CO_2 flux in the sub-Antarctic Ocean. Tellus Ser. B 51, 849-861, doi: 10.1034/j.1600-0889.1999.t01-3-00008.x.

Moore, C.M., Suggett, D., Holligan, P.M., Sharples, J., Abraham, E.R., Lucas, M.I., Rippeth, T.P., Fisher, N.R., Simpson, J.H., Hydes, D.J., 2003. Physical controls on phytoplankton physiology and production at a

shelf sea front: a fast repetition-rate fluorometer based field study. Mar. Ecol. Prog. Ser. 259, 29-45, doi: 10.3354/meps259029.

Moore, J.K., Abbott, M.R., 2000. Phytoplankton chlorophyll distributions and primary production in the Southern Ocean. J. Geophys. Res. 105, 28709-28722, doi: 10.1029/1999JC000043.

Ogren, W.L., 1984. Photorespiration: Pathways, regulation, and modification. Annu. Rev. Plant Physiol. Plant Mol. Biol. 35, 415-442.

Olaizola, M., Yamamoto, H.Y., 1994. Short-term response of the diadinoxanthin cycle and fluorescence yield to high irradiacnce in *Chaetoceros muelleri* (Bacillariophyceae). J. Phycol. 30, 606-612, doi: 10.1111/j.0022-3646.1994.00606.x.

Olson, R.J., Sosik, H.M., Chekalyuk, A.M., Shalapyonok, A., 2000. Effects of iron enrichment on phytoplankton in the Southern Ocean during late summer: active fluorescence and flow cytometric analyses. Deep-Sea Res. Pt. II 47, 3181-3200, doi: 10.1016/S0967-06450000064-3.

Platt, T., Gallegos, C.L., Harrison, W.G., 1980. Photoinhibition of Photosynthesis in Natural Assemblages of Marine-Phytoplankton. J. Mar. Res. 38, 687-701.

Prasil, O., Kolber, Z., Berry, J.A., Falkowski, P.G., 1996. Cyclic electron flow around photosystem II in vivo. Photosynth. Res. 48, 395-410, doi: 10.1007/BF00029472.

Raateoja, M., Seppala, J., Kuosa, H., 2004. Bio-optical modelling of primary production in the SW Finnish coastal zone, Baltic Sea: fast repetition rate fluorometry in Case 2 waters. Mar. Ecol. Prog. Ser. 267, 9-26, doi: 10.3354/meps267009.

Rintoul, S.R., Trull, T.W., 2001. Seasonal evolution of the mixed layer in the Subantarctic Zone south of Australia. J. Geophys. Res. 106, 31447-31462, doi: 10.1029/2000jc000329.

Sarmiento, J.L., Gruber, N., Brzezinski, M.A., Dunne, J.P., 2004. High-latitude controls of thermocline nutrients and low latitude biological productivity. Nature 427, 56-60, doi: 10.1038/nature02127.

Sarmiento, J.L., Hughes, T.M.C., Stouffer, R.J., Manabe, S., 1998. Simulated response of the ocean carbon cycle to anthropogenic climate warming. Nature 393, 245-249, doi: 10.1038/30455.

Sedwick, P.N., Edwards, P.R., Mackey, D.J., Griffiths, F.B., Parslow, J.S., 1997. Iron and manganese in surface waters of the Australian subantarctic region. Deep-Sea Res. Pt. I 44, 1239-1253, doi: 10.1016/S0967-06379700021-6.

Smyth, T.J., Pemberton, K.L., Aiken, J., Geider, R.J., 2004. A methodology to determine primary production and phytoplankton photosynthetic parameters from Fast Repetition Rate Fluorometry. J. Plankton Res. 26, 1337-1350, doi: 10.1093/plankt/fbh124.

Strutton, P.G., Griffiths, F.B., Waters, R.L., Wright, S.W., Bindoff, N.L., 2000. Primary productivity off the coast of East Antarctica (80-150°E): January to March 1996. Deep-Sea Res. Pt. II 47, 2327-2362, doi: 10.1016/S0967-06450000028-X.

Suggett, D., Kraay, G., Holligan, P., Davey, M., Aiken, J., Geider, R., 2001. Assessment of photosynthesis in a spring cyanobacterial bloom by use of a fast repetition rate fluorometer. Limnol. Oceanogr. 46, 802-810.

Suggett, D.J., Moore, C.M., Oxborough, K., Geider, R.J., 2005. Fast repetition rate (FRR) chlorophyll a fluorescence induction measurements. Chelsea Technologies Group, Surrey.

Sullivan, C.W., Arrigo, K.R., Mcclain, C.R., Comiso, J.C., Firestone, J., 1993. Distributions of Phytoplankton Blooms in the Southern-Ocean. Science 262, 1832-1837, doi: 10.1126/science.262.5141.1832.

Vaillancourt, R.D., Sambrotto, R.N., Green, S., Matsuda, A., 2003. Phytoplankton biomass and photosynthetic competency in the summertime Mertz Glacier Region of East Antarctica. Deep-Sea Res. Pt. II 50, 1415-1440, doi: 10.1016/S0967-06450300077-8.

Westwood, K.J., Webb, J., Griffiths, F.B., Wright, S.W., 2011. Primary production in the Sub-Antarctic and Polar Frontal zones south of Tasmania, Australia; SAZ-Sense survey, 2007. Deep-Sea Res. Pt. II, this issue.

Williams, P.J.L., Robinson, C., Sondergaard, M., Jespersen, A.M., Bentley, T.L., Lefevre, D., Richardson, K., Riemann, B., 1996. Algal ^{14}C and total carbon metabolisms. 2. Experimental observations with the diatom *Skeletonema costatum*. J. Plankton Res. 18, 1961-1974, doi: 10.1093/plankt/18.10.1961.

Wright, S.W., Thomas, D.P., Marchant, H.J., Higgins, H.W., Mackey, M.D., Mackey, D.J., 1996. Analysis of phytoplankton of the Australian sector of the Southern Ocean: Comparisons of microscopy and size frequency data with interpretations of pigment HPLC data using the 'CHEMTAX' matrix factorisation program. Mar. Ecol. Prog. Ser. 144, 285-298, doi: 10.3354/meps144285

Wright, S.W., van den Enden, R.L., Pearce, I., Davidson, A.T., Scott, F.J., Westwood, K.J., 2010. Phytoplankton community structure and stocks in the Southern Ocean (30-80°E) determined by CHEMTAX analysis of HPLC pigment signatures. Deep-Sea Res. Pt. II, 57, 758-778, doi: 10.1016/j.dsr2.2009.06.015.

List of Tables

List of Figures

Figure 2 Vertical profiles of F_v/F_m, F_q'/F_m', q_P, σ_{PSII}' and E obtained from two FRRF casts at Station 4. (a) and (b) were data from CTD 12 collected at dawn while (c) and (d) were midday measurements from CTD 18.

Figure 3 Vertical profiles of chl *a*, FRRF-based PP, photochemical efficiency and macronutrients at the three process stations. P1, Process station 1; P2, Process station 2; P3, Process station 3

Figure 4 Comparison between primary productivity measured by FRRF and ^{14}C for (a) all stations (r^2 = 0.85, slope = 1.23±0.05 s.d., n = 85, P < 0.01), (b) under light limitation conditions (r^2 = 0.96, slope = 1.05±0.03 s.d., n = 71, P < 0.01) and (c) under light saturation conditions (r^2 = 0.64, slope = 1.43±0.23 s.d., n = 14, P < 0.01). The dashed line represents the 1:1 relationship. T1, Transit 1; P1, Process 1; P2, Process 2; T3, Transit 3; P3, Process 3; T4, Transit 4

Figure 5 Correlation between the (a) chl *a*-specific rate of electron transfer (ETR^{chl}) and the carbon uptake rate per unit chl *a* (P^B) for all stations (r^2 = 0.74, slope = 5.07±0.28 s.d., n = 85, P < 0.01), (b) FRRF- and ^{14}C-derived primary productivity normalised by light for all stations (r^2 = 0.86, slope = 1.03±0.00 s.d., n = 85, P < 0.01). The dashed line represents the 1:1 relationship.

Figure 6 Relationship between FRRF- and ^{14}C-based primary productivity measurements at (a) P1 (SAZ-West) (r^2 = 0.98, slope = 0.79±0.06 s.d., n = 19, P < 0.01), (b) P2 (PFZ) (r^2 = 0.97, slope = 1.67±0.11 s.d., n = 6, P < 0.01). and (c) P3 (SAZ-East) (r^2 = 0.92, slope = 1.43±0.10 s.d., n = 14, P < 0.01).. The dashed line represents the 1:1 relationship. P, Process station; SAZ, Sub-Antarctic Zone; PFZ, Polar Frontal Zone

Figure 1

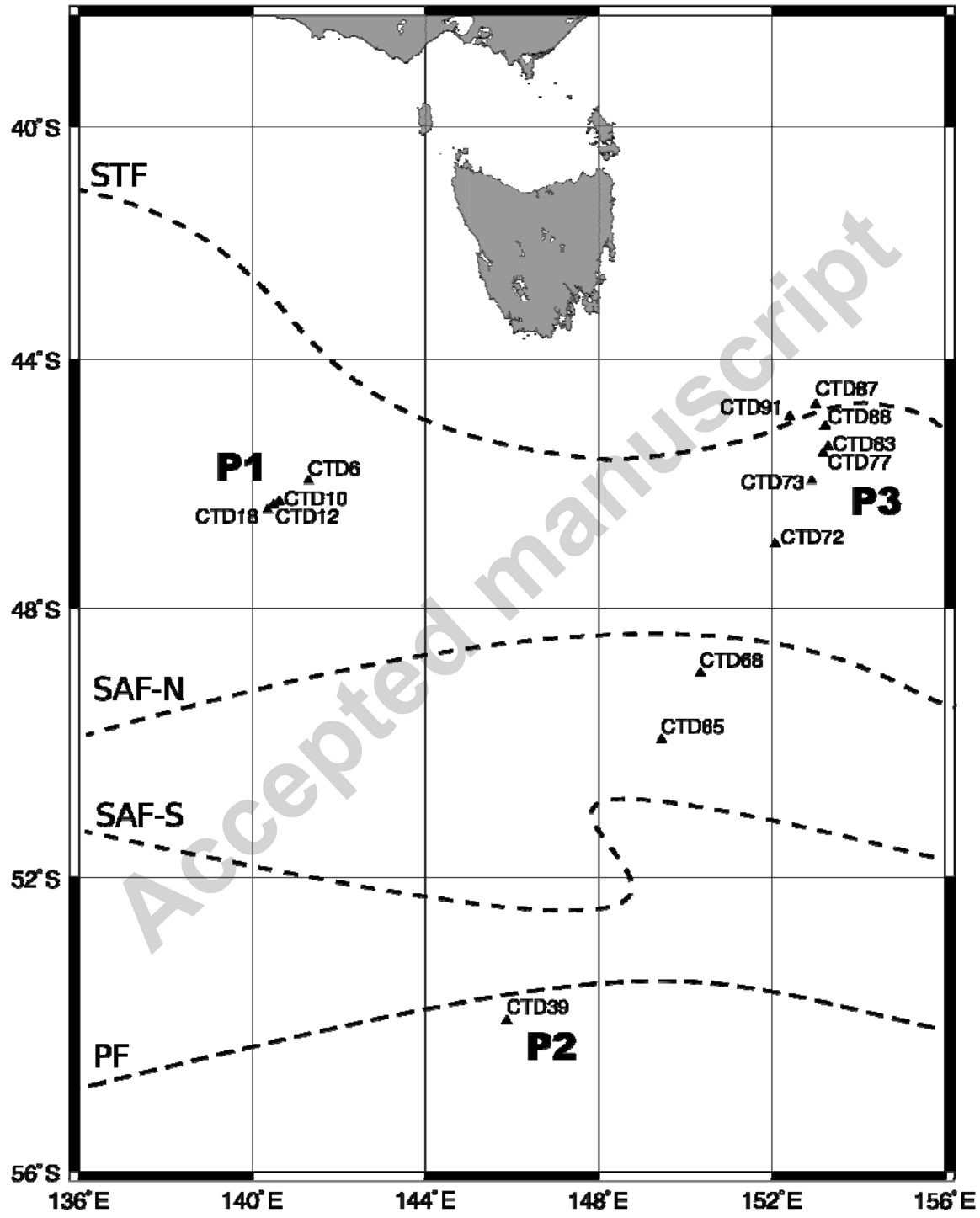

Figure 2

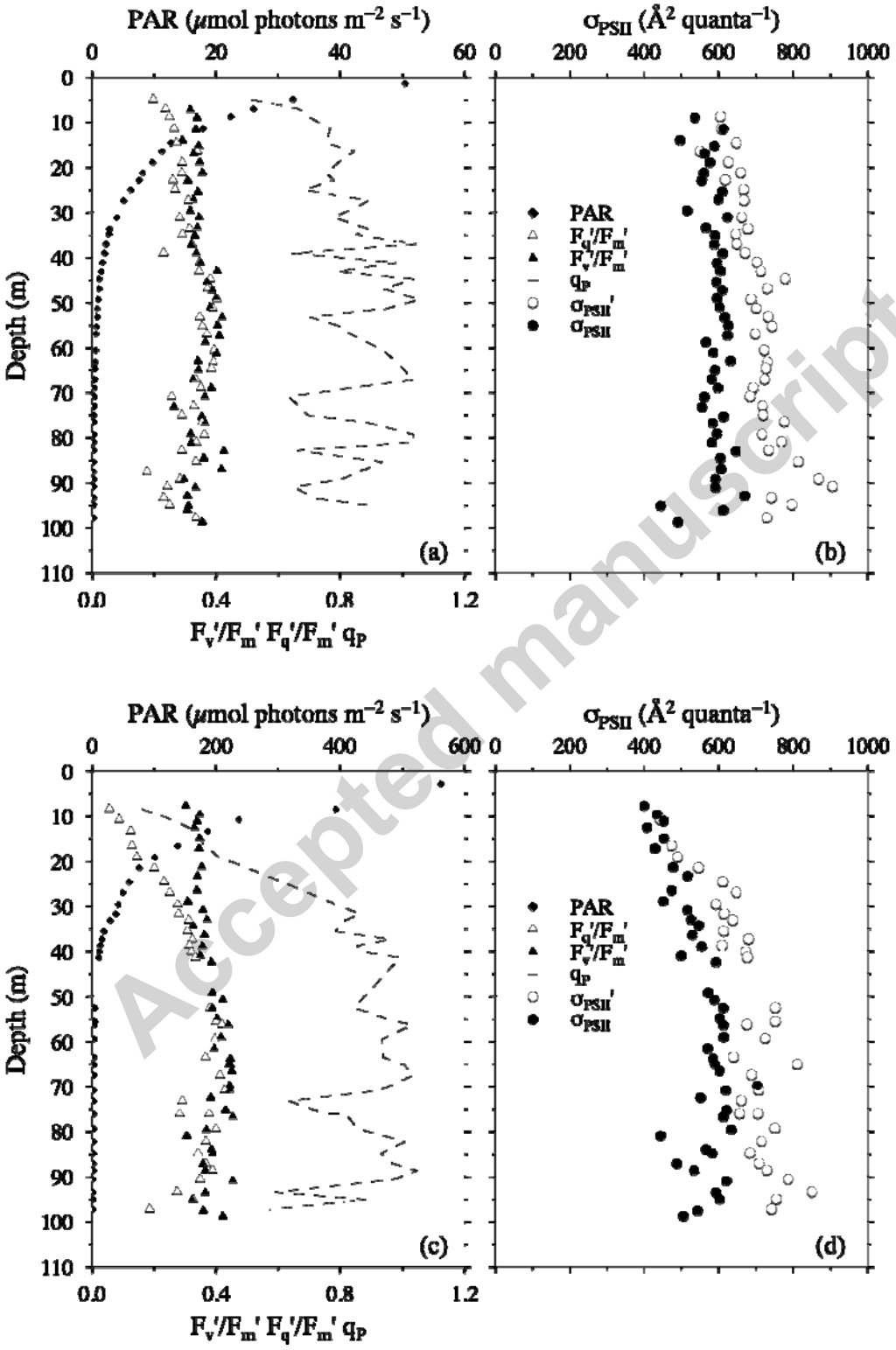

Figure 3

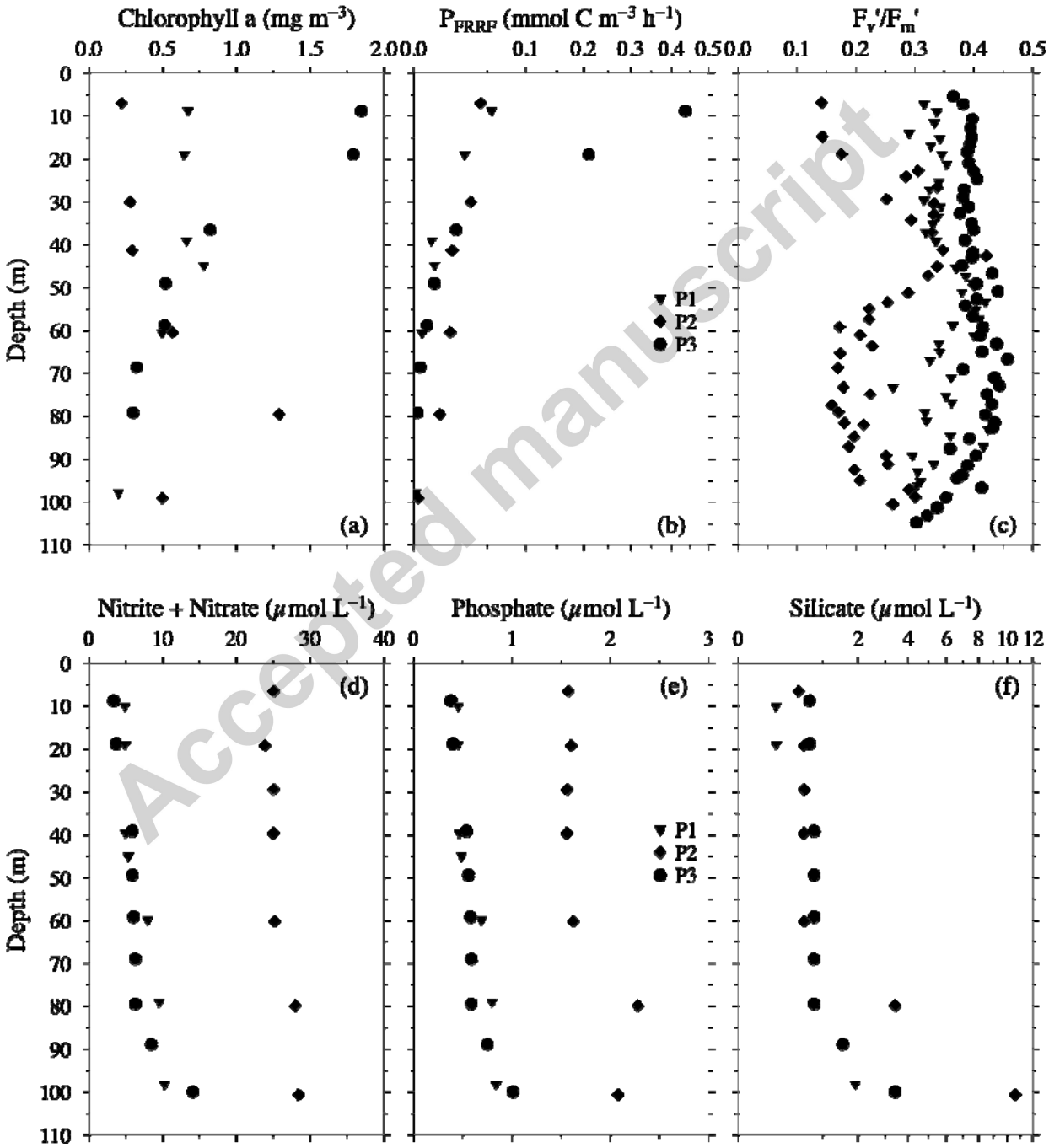

Figure 4

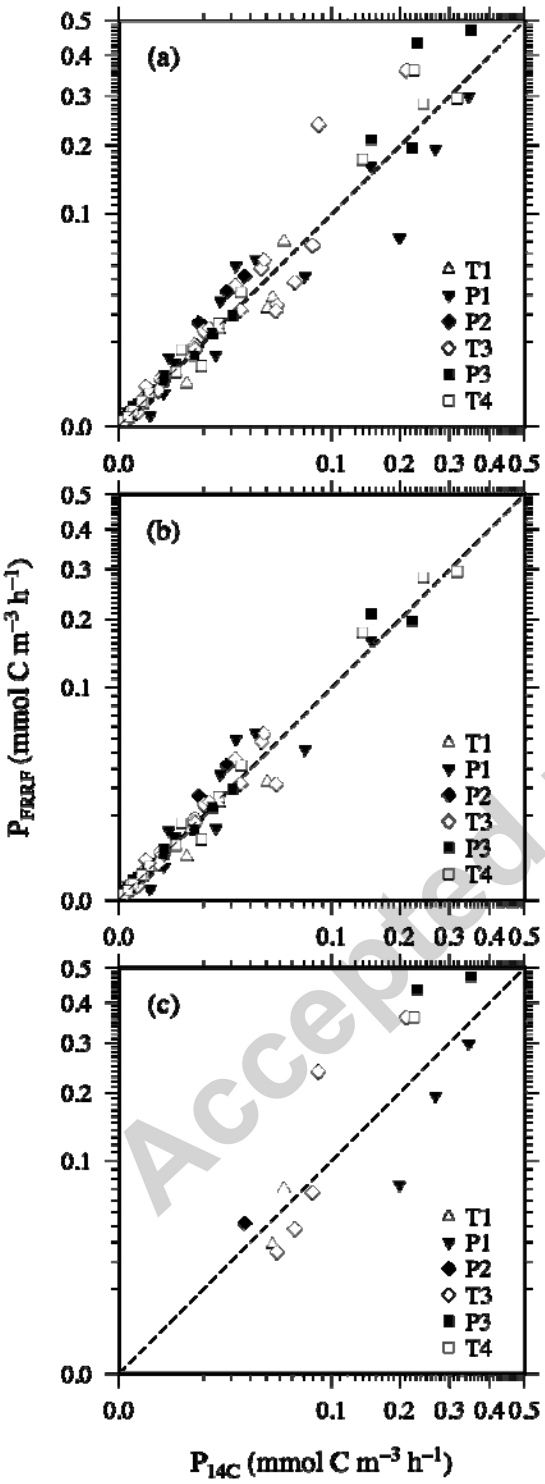

Figure 5

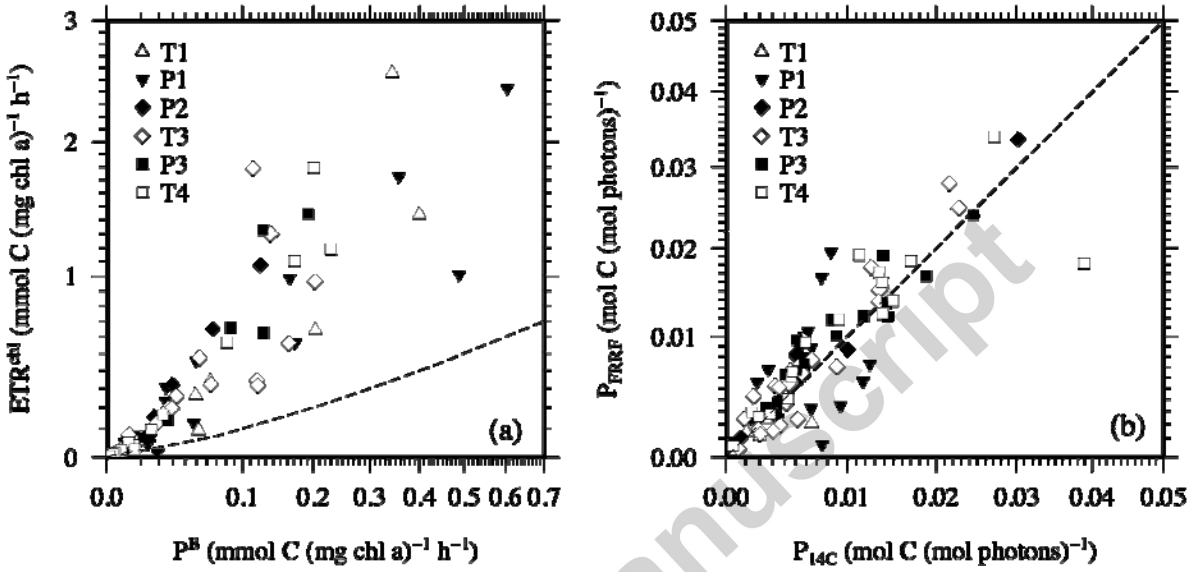

Figure 6

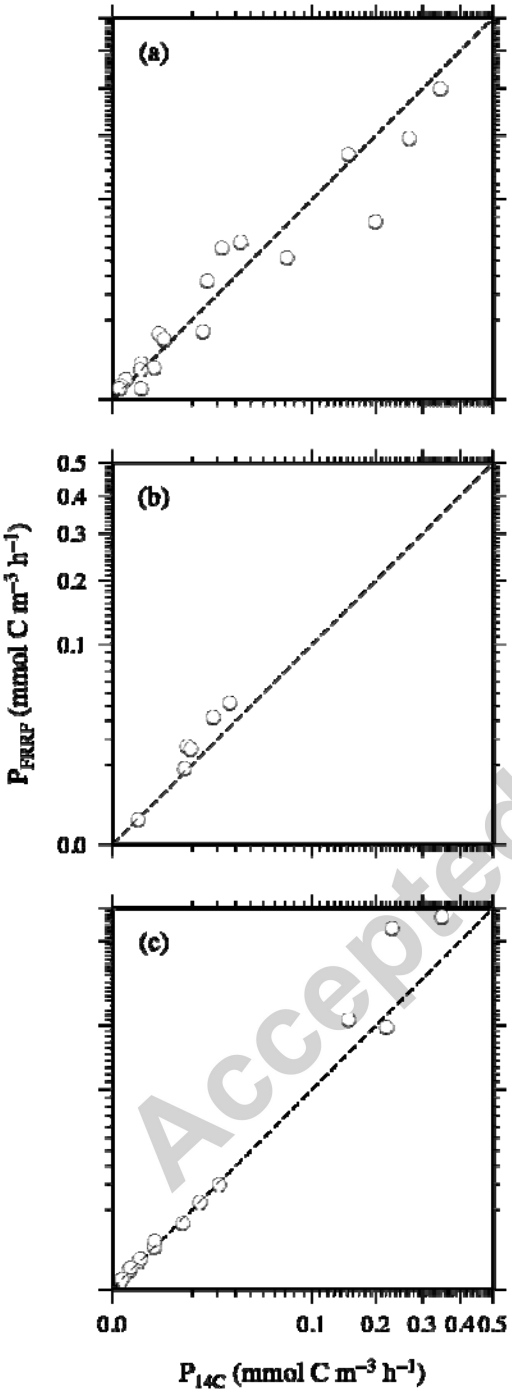

1 Table 1

Zone	SAZ	SAZ	SAZ	SAZ	PF	SAZ	SAZ	SAZ	SAZ	SAZ/STF	SAZ	SAZ	SAZ	SAZ
Transit & Process	T1	P1	P1	P1	P2	T3	T3	T3	T3	P3	P3	T4	T4	T4
Station	3	4	4	4	6	10	11	13	14	17	17	18	19	21
CTD	6	10	12	18	39	65	68	72	73	77	83	87	88	91
Time and Date (local)	1147 21-Jan-07	1254 22-Jan-07	0658 23-Jan-07	1341 24-Jan-07	1658 1-Feb-07	1459 8-Feb-07	0832 9-Feb-07	1054 10-Feb-07	1717 10-Feb-07	1244 11-Feb-07	1341 12-Feb-07	1329 13-Feb-07	1716 13-Feb-07	0912 14-Feb-07
Latitude	45°59′S	46°19′S	46°23′S	46°27′S	54°0′S	50°0′S	48°59′S	46°59′S	45°59′S	45°32′S	45°26′S	44°45′S	45°6′S	44°56′S
Longitude	141°17′E	140°37′E	140°28′E	140°21′E	145°52′E	149°26′E	150°20′E	152°4′E	152°54′E	153°10′E	153°17′E	153°0′E	153°13′E	152°23′E
Mixed layer depth (m)	27	25	43	46	49	67	69	63	18	16	17	27	30	25
Stratification	Active mixing	Active mixing	Active mixing	Active mixing	Low mixing	Low mixing	Low mixing	Low mixing	Active mixing	Active mixing	Active mixing	Active mixing	Active mixing	Active mixing
Sea surface temperature (°C)	12.4	13.1	12.9	12.8	5.5	9.5	9.5	12.8	13.3	13.5	13.5	14.9	14.7	15.0
Sea surface salinity	34.7	34.7	34.7	34.7	33.8	34.2	34.3	34.9	34.7	34.9	34.8	35.2	35.2	35.2
Chl *a* concentration (mg m^{-3})	0.11	0.45	0.67	0.97	0.22	0.38	0.39	1.56	0.75	1.83	1.85	1.43	1.13	1.38

Surface FRRF-based PP (mmol C m^{-3} h^{-1})	0.028	0.193	0.055	0.299	0.042	0.038	0.022	0.360	0.238	0.471	0.436	0.282	0.360	0.293
Surface ^{14}C-based PP (mmol C m^{-3} h^{-1})	0.044	0.269	0.033	0.346	0.027	0.062	0.046	0.211	0.084	0.350	0.231	0.244	0.225	0.316

2

3 Table 2

Parameter	Definition	Units
E	Irradiance	μmol photons $m^{-2}s^{-1}$
F_o, F_m	Minimum and maximum fluorescence in dark-adapted state	Dimensionless
F_o', F', F_m'	Minimum, steady state and maximum fluorescence under ambient light	Dimensionless
F_v	Variable fluorescence under in dark-adapted state ($F_m - F_o$)	Dimensionless
F_v'	Variable fluorescence under ambient light ($F_m' - F_o'$)	Dimensionless
F_q'	Difference between Fm′and F'($F_m' - F'$) under ambient light	Dimensionless
F_v/F_m	Maximum photochemical efficiency	Dimensionless
F_v'/F_m'	Maximum photochemical efficiency under ambient light	Dimensionless
F_q'/F_m'	Photochemical efficiency under ambient light	Dimensionless
q_P or F_q'/F_v'	Photochemical quenching or PSII efficiency factor under ambient light	Dimensionless
σ_{PSII}	Effective absorption cross section of PSII in dark-adapted state	$Å^2$ $quanta^{-1}$
σ_{PSII}'	Effective absorption cross section of PSII under ambient light	$Å^2$ $quanta^{-1}$
n_{PSII}	Photosynthetic unit size of PSII reaction centres	mol RCII (mol chl a)$^{-1}$
$1/k$	Quantum yield of electron transport through PSII per O_2 molecule evolved	mol O_2 (mol photons)$^{-1}$
PQ	Photosynthetic quotient	mol O_2 evolved (mol C fixed)$^{-1}$

4

5